

Microencapsulation of Drugs for Biodegradable Coatings

Inês Quinta Queimada de Jesus Rosa
inesjrosa@ist.utl.pt
Instituto Superior Técnico, Lisboa, Portugal

October 2021

Abstract

Magnesium (Mg) alloys have been studied for biomedical applications. In the present work, two types of microcapsules (MCs) were produced: PCL (poly(ϵ -caprolactone) and polylactic acid (PLA) microcapsules loaded with ibuprofen and calcium, respectively. The encapsulation process aims to control the release of the active compounds, through the protective polymer shell.

Relatively high encapsulation yields, between 55.9% and 76.1%, were obtained. The use of lower polymer concentration (16.7 wt% PCL, 16.7 wt% PLA) and higher volume ratio of external aqueous phase (W_2) resulted in smaller core-shell MCs (between $69.8 \mu\text{m} \pm 34.2$ and $235 \mu\text{m} \pm 169$) with higher encapsulation yield. Fourier Transform Infrared Spectroscopy (FTIR), Ultraviolet-Visible Spectroscopy (UV-Vis) and Atomic Absorption Spectroscopy (AAS) results showed that MCs were successfully prepared. Different synthesis parameters resulted in different MCs' morphologies, studied by optical microscopy and SEM analysis. The release rate profile of ibuprofen showed an initial burst release, followed by a non Fickian diffusion mechanism (Super Case-II transport). Electrochemical Impedance Spectroscopy (EIS) revealed that the presence of MCs in different aqueous media (MEM, NaCl and PBS) did not impact the corrosion rate of the Mg alloy, which allow us to conclude that they are a promising anti-inflammatory strategy, when incorporated in coatings of metallic biodegradable implants.

Keywords: Microencapsulation, Biodegradable, Ibuprofen, Calcium, Polycaprolactone

1. Introduction

The preparation of bio-functional coatings containing drug-loaded microcapsules can not only improve the corrosion resistance of Mg alloys, but also provide anti-inflammatory properties through the release of anti-inflammatory agents. This thesis will focus on the production of biodegradable microcapsules, their associated controlled drug release and their effect on degradable metal alloys used in biomedical applications.

Different types of metals have been used in bio-applications and it is possible to divide them into groups: Stainless Steel alloys, Cobalt-Chromium alloys and Titanium and its alloys [1]. However, drawbacks associated with the use of these materials are: incompatibility of mechanical properties of the metallic alloys and natural bone that can lead to stress shielding, mechanical wear and corrosion, that results from the long-term implantation in the body, and consequent release of toxic metal ions that may reduce the biocompatibility of implants [2][3]. Furthermore, the need to surgically remove the implant after healing increases associated health risks and costs.

Biodegradable materials, designed to degrade over a predetermined implantation period when exposed to biological activity, appeared as an alterna-

tive to traditional biomedical metallic biomaterials [4][5][6]. Over time, the metallic elements used need to be metabolized by the human body and need to have an appropriate degradation rate and mode in the environment of application [6][7][8]. Mg and its alloys have been gaining interest from biomedical applications since this material is lightweight, exhibits good mechanical properties, higher fracture toughness than ceramic materials and an elastic modulus and compressive yield strength similar to those of natural bone. In addition, Mg is biocompatible and essential to human metabolism as it is one of the most abundant ions in the human body, mostly stored in bone tissue [9][10]. However, Mg and its alloys' application is limited due to a low corrosion resistance that results in an uncontrolled and fast degradation [9][10]. Limitations due to the high corrosion rate at physiological pH (7.4-7.6), resulting in the formation of H_2 gas can lead to balloon effect in vivo if rapidly absorbed. Another concern for biomedical applications of Mg alloys is the local increase of pH near the corrosive surface [2].

To regulate the uncontrolled fast corrosion of Mg, their composition can be optimized via alloying, or polymeric coatings to improve the corrosion behaviour [2]. Coatings are mainly applied on surfaces

for functional or protective purposes [11]. Besides corrosion resistance of Mg alloys, polymer coatings also provide diverse functionalities such as improved biocompatibility, self-healing, drug-delivery ability, osteoinduction, hydrophobicity and antibacterial performance [12]. Controllable biodegradability achieved by the utilization of coatings reduces the risk of implant failure in the early implantation period.

2. Background

Microencapsulation consists of a process in which micron sized solid, gases or liquids are entrapped by a continuous film of polymeric material [13][14][15].

Microcapsules' sizes can range from 1 μm to a few millimeters leading to large surface areas. This characteristic allows several chemical reactions to occur on the surface area such as absorption, desorption, light scattering, etc [13][16]. Throughout the years, the technology of microencapsulation has been applied to many fields (pharmaceutical, agricultural, oil industries, food industries, etc.) since it has been generally accepted as a way to protect drugs from the surrounding environment and as systems for controlled release of drugs [17]. Microencapsulation technology can be used to obtain five different objectives: immobilization or entrapment, protection, controlled release, structuration and functionalisation [18].

This technique ensures the protection of the encapsulated material from the surrounding environment until it reaches the area of action, being used to stabilize sensitive substances (providing protection against chemical, physiochemical and mechanical environmental conditions). It also provides a controlled release of the active compound and allow the conversion of liquids into free flowing solids, to separate and eliminate incompatible components [13][14][18].

Microencapsulation is a versatile, stable and customizable technique when compared to other controlled release systems (nanoparticles, vesicles or cells). It becomes an interesting alternative to provide safe and effective delivery of drugs and biomolecules [19]. In pharmaceutical and biomedical applications, there's an additional concern in the production of microcapsules, associated with the need to guarantee biocompatibility and the need to focus on sustained and targeted release of drugs.

Ibuprofen is a non-steroidal anti-inflammatory drug (NSAID) with anti-inflammatory, analgesic and antipyretic effects [20][21]. It is used to relieve mild to moderate symptoms of pain related with rheumatoid arthritis, primary dysmenorrhea, headaches, migraines and soft tissue disorders [22][23]. It is a widely used medication as it is generally tolerated and is considered to be one of the safest

NSAIDs. Nevertheless, ibuprofen may cause some unwanted effects. The most commonly reported are nausea, vomiting, decreased hemoglobin and hypertension, but also ulcers and dyspepsia [24][25][26]. Although there's no evidence of serious long-term adverse effects, NSAIDs can induce gastrointestinal side effects. A study from 2010 established a relationship between the regular use of NSAIDs and an increased hearing loss [25]. Better performance and less severe secondary effects of NSAIDs can be controlled by the type of drug delivery system. Optimal delivery systems need to ensure drug delivery over an extended period of time, with a controlled and sustained release profile [27].

Microcapsules or microspheres as drug carriers allow the control of the drug release profile in the time interval until the target is reached [25][27]. Drug release from microcapsules can occur via three mechanisms: diffusion, chemical reaction and solvent activation [28].

For small encapsulated molecule drugs, diffusion is the most common release mechanism since the molecules migrate from within the polymer deposit to the surface area and then to the outside media. Diffusion as a release mechanism is dependent on the size of the encapsulated molecule and the size of the polymer reservoir, since molecules need to diffuse through polymeric materials [28][29].

Drug release by chemical reaction consists of the erosion and degradation of polymeric matrices. The hydrolysis of individual polymer chains, to lower molecular weight molecules, describes a degradation process while erosion is related to the mass loss from the polymer matrix. In commonly used biodegradable polymers, surface erosion and bulk erosion can occur [28].

Swelling of polymer or osmotic effects correspond to a solvent activation release mechanism. Osmotic potential gradients, across polymer barriers, generate pressurized chambers containing aqueous solutions of the encapsulated material. The flow of said solution relieves the pressure out of the delivery device [28][29].

The control of drug distribution in drug delivery systems is of great importance. This is achieved via precise drug delivery systems to minimize the side effect of drugs [25]. Different types of diffusion kinetics are depicted in four theoretical curves presented in Figure 1. The different types of release behaviour are plotted as percentage of drug release over time [25][30].

Plot A illustrates a constant rate release, representing the release of encapsulated material of a non-erodible, spherical MC by steady-state diffusion through a uniform coating. Curve B shows a similar release behaviour as A with an initial burst release. Curve C represents a linear

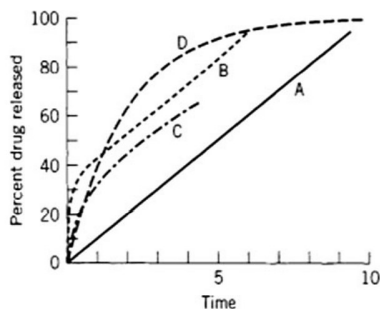


Figure 1: Theoretical curves of release behaviour. Curve A - Spheric microcapsule free of lag time and burst effects; Curve B - Equal to curve A with burst effects; Curve C - Matrix or monolithic sphere with square root time release; Curve D - First order kinetics [25][30].

plot between the percentage of drug release and the square-root of time. In this case, the Higuchi model ($F = K_H \cdot t^{0.5}$) is valid up to 60% release if the microsphere acts as a matrix of inert particles where the core material is dispersed. Curve D represents a first order release, when the plot of the logarithm of the percentage of non-released core material as a function of time is linear [25][30].

Various mathematical models were developed to describe drug release from polymeric systems, from simple empirical models, such as the Higuchi equation and Korsmeyer–Peppas model, to more complex models that account the simultaneous diffusion, swelling and dissolution processes [25][30]. Korsmeyer–Peppas’s model describing the release of drugs from polymeric systems is represented by:

$$\frac{M_t}{M_\infty} = K \cdot t^n \quad (1)$$

where M_T/M_∞ corresponds to the ratio between the percentage of drug released at each time point and the percentage of release at equilibrium. K is the constant of drug release, t is the time measured and n is the diffusion exponent [25][30]. The diffusion exponent is indicative of the mechanism of drug release. For spherical geometry, if n is equal to 0.85, the rate of drug release is independent of time (zero order kinetics). This mechanism is denominated as Case-II transport [25][30]. In this case, the rate-controlling step is the relaxation process of macromolecules due to the imbibition of water in the system. The glass temperature of the polymer decreases since the water acts as a plasticizer and once T_g equals the set temperature, the polymer chains transfer from a glassy to a rubbery state with associated volume expansion and increased mobility of macromolecules [25][30]. Applying Eq. 1 for

spherical geometries, two special cases occur at $n = 0.43$ (diffusion controlled drug release) and at $n = 0.85$ (swelling controlled drug release). Diffusion exponents between 0.43 and 0.85 represent anomalous transport which can be regarded as a superposition of both phenomena (Table 1).

Table 1: Diffusion coefficient values and respective drug delivery models [25].

Plane Surface	Cylinder	Sphere	Drug Delivery systems
0.5	0.45	0.43	Fickian diffusion mechanism
$0.5 < n < 1.0$	$0.45 < n < 0.89$	$0.43 < n < 0.85$	Anomalous diffusion
1.0	0.89	0.85	Non-Fickian diffusion mechanism

3. Materials and Methods

3.1. Materials

Ibuprofen 99% and calcium chloride 96% were supplied by Alfa Aesar and used without chemical purification. Poly(ϵ -caprolactone) average Mw 45000 g/mol from Sigma-Aldrich, Polylactic Acid from BASF, Dichloromethane (DCM) 99.8% supplied by Fisher Chemical, Polyvinyl alcohol (PVA) 98-99% from Alfa Aesar and Gum Arabic from Fisher Chemical.

3.2. Preparation of ibuprofen microcapsules

Microencapsulation was achieved via double emulsion of water in oil in water ($W_1/O/W_2$), where W_1 phase consists of Ibuprofen dissolved in 2-propanol (15 wt%; 30 wt% or 40 wt%), organic phase of PCL in DCM (16.7 wt%) and W_2 phase of 4 wt% PVA solution and gum Arabic.

Microcapsules with three increasing concentrations of ibuprofen were prepared, the overall concentration of ibuprofen in the prepared MCs was 16 wt%, 28 wt% or 34 wt%.

The simple emulsion ($W1/O$) is formed at room temperature by mechanical stirring with an IKA T 18 digital Ultra-Turrax, Germany, at 7800 rpm for 5 minutes. Afterwards, the double emulsion is generated by adding the simple emulsion to a continuous phase W_2 under mechanical stirring (Heidolph RZR 2102 control for medium-high viscosity liquids with a stirring shaft with turbo propeller from VELP Scientifica) at 610 rpm for 2.5 hours until total evaporation of the the solvent, at room temperature. Once the microencapsulation process was complete, the formed MCs were filtered under vacuum and washed with water. After filtration process the microcapsules were left to dry for 48h at environmental conditions.

3.3. Preparation of ibuprofen and calcium microcapsules

Microencapsulation via double emulsion of water in oil in water ($W_1/O/W_2$), where W_1 consists of

ibuprofen and calcium in 2-propanol, O phase comprises PLA (16.7 wt%) in DCM and W_2 a 4 wt% PVA solution and gum Arabic. The experimental process followed is equal to the one described for the preparation of ibuprofen microcapsules.

3.4. Characterization

Optical Microscopy

A Kruss MSZ 5600 optical microscope (Hamburg, Germany) was used to evaluate the emulsion stability and the size of the microcapsules produced. Shell maturity was also evaluated during the synthesis process, in order to perform a qualitative evaluation of the MCs' shell stiffness.

Scanning Electron Microscopy (SEM)

The microcapsules produced were assessed by SEM to evaluate their morphology, roughness, porosity and size. This analysis was carried out with a JEOL JSM7001F (JEOL, Tokyo, Japan) field emission gun scanning electron microscope (FEG-SEM) operating at 15 kV. Before the analysis, conductive double-sided adhesive tape was applied to immobilize the samples in a sample holder. These were then coated with a conductive Au/Pd thin film, through sputtering using a Quorum Technologies sputter coater, model Q150T ES (Lewes Road, Laughton, UK).

Fourier transform infrared spectroscopy

FTIR spectroscopy was used to assess the chemical structure of the molecules by identifying specific characteristic groups, leading to the identification of the compounds present in the shell and core of the analysed microcapsules [31]. The equipment used was a PerkinElmer Spectrum Two FTIR spectrometer equipped with a Pike Technologies Miracle Attenuated Total Reflectance (ATR) accessory. The spectra were obtained at 4 cm^{-1} resolution and 8 scans of data accumulation.

Thermogravimetric Analysis (TGA)

Through the thermograms and derivative curves (DTG) obtained in thermogravimetric analysis it is possible to quantify the amount of encapsulated material and to evaluate the thermal stability of a material by observing the variation of mass with the increase of temperature. Thermogravimetric Analysis was performed using a Hitachi STA 7200 Thermal Analysis System (Ibaraki, Japan) under a controlled nitrogen atmosphere with a flow of 200 mL/min, at a heating rate of $10\text{ }^\circ\text{C}/\text{min}$, in the range of 25-600 $^\circ\text{C}$.

Drug Release Analysis

To analyse the kinetic release of ibuprofen and/or calcium, a suspension of 100 mg of MCs in 200 mL of deionized water was prepared, in triplicate, and stirred continuously for 24 hours.

The drug release profile consists of a plot of the concentration of the drug as a function of time (prede-

termined intervals at which samples are retrieved). The removed volume was replaced with fresh deionized water.

UV/Vis Spectroscopy

The ibuprofen released from the MCs was quantitatively determined by UV/Vis Spectrophotometer (Shimadzu UV-3100 equipment with UVProbe 2.10 software) using Lambert Beer's law that establishes a linear relationship between the absorbance (Abs) and the concentration (C). A spectrum from 200-400 nm was obtained and maximum absorbance at 222 nm was studied.

Atomic Absorption Spectroscopy (AAS)

AAS is a technique based on the principle that free atoms from an atomizer, absorb radiation at specific wavelengths. To determine the amount of encapsulated calcium, an Avanta GBC Scientific equipment was used, knowing that calcium atoms absorb energy of 422.7 nm [32][33].

Electrochemical Impedance Spectroscopy

EIS analyses the impedance of a corroding metal as a function of frequency. Electrochemical Methods in alternating-current circuits can provide insights into corrosion mechanisms and/or on the effectiveness of corrosion control methods [34][35].

EIS measurements were performed in a three-electrode cell with the Mg alloy sample as the working electrode, a SCE as the reference electrode and a platinum foil counter electrode. To avoid interference of external electromagnetic fields, the cell was placed in a Faraday cage. Three different electrolytes were used: 0.05 M NaCl aqueous solution, 10 mM PBS aqueous solution and minimum essential medium (MEM). Measurements were performed using a Gamry FAS2 Fentostat with PCI4 Controller. Scanning frequency ranged from 10^5 to 10^{-2} Hz with a 10 mV rms sinusoidal perturbation with 7 points per frequency decade. Scans were performed at different immersion times and all spectra was recorded at open circuit potential.

4. Results

Different methods of microencapsulation via solvent evaporation and different processing conditions were tested to evaluate the adequate method to produce the desired MCs. The MCs formulation process with double emulsion combined with solvent evaporation method ($W_1/O/W_2$) allowed the evaluation of crucial parameters of the synthesis such as polymer concentration, volume of W_2 phase and solvent used in W_1 phase.

Initially, empty microcapsules were produced and smaller sized microcapsules were obtained with lower concentrations of PCL as the shell-forming polymer. Higher polymer concentrations led to the production of microcapsules of larger size and concentrations as high as 25 wt% of PCL did not pro-

duce viable microcapsules. The higher the polymer concentration the higher the viscosity of O phase of the emulsion system which might compromise the homogeneity of this phase and cause problems in the stability of the emulsion and, consequently, may result in a broader size distribution of MCs.

The second variable under analysis was the solvent (water, 1-propanol and 2-propanol) used in phase W_1 , where the encapsulated material would be dissolved. MCs prepared with 1-propanol have smaller average size with uniform spherical shape. Sample produced with 2-propanol as a solvent presents a vast and generalized size distribution and microcapsules produced with water have, simultaneously, the smaller polydispersity index and the largest capsule size.

The last variable in study corresponds to the volume of the external aqueous phase. An increase of W_2 phase volume and the use of 1-propanol allowed the preparation of spherical and small microcapsules but the process with lower W_2 volume has a higher process yield and resulted in microcapsules with a smaller size.

Another method of microencapsulation was tested, consisting of a simple oil in water emulsion (O/W). Different compositions of phase W were tested to understand its impact on the stability of the emulsion and on the final prepared MCs. MCs formulation using higher concentration of PVA led to loose, disaggregated and mostly spherical MCs. Gum Arabic in the aqueous phase led to a majority of spherical MCs however, larger MCs seem to be flat with a round shape. Although the synthesis process with gum Arabic in phase W has a lower yield, it allows the preparation of a more monodisperse and homogeneous sample with MCs of smaller sizes.

Ibuprofen Microcapsules

Microcapsules encapsulating three different concentrations of ibuprofen, 16 wt%, 28 wt%, 34 wt%, were prepared and are designated as IBU_16, IBU_28 and IBU_34, respectively.

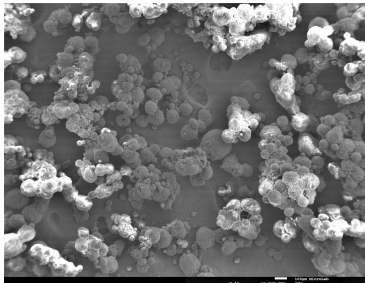


Figure 2: SEM images of IBU_16 MCs.

Figures 2, 3 and 4 show SEM images that allowed the assessment of MCs' morphology, shell thickness and size distribution.

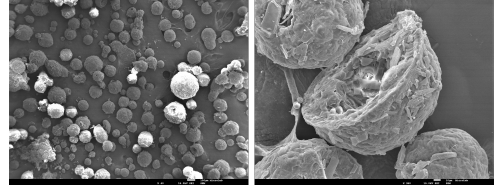


Figure 3: SEM images of IBU_28 MCs.

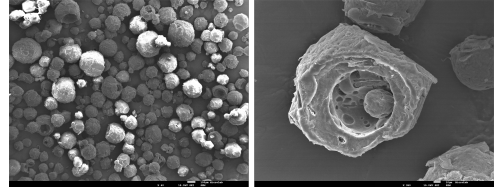


Figure 4: SEM images of IBU_34 MCs.

Every synthesis led to the preparation of microcapsules with spherical core-shell morphologies however, thick shells are observed (Figure 3 and 4). Higher concentrations of ibuprofen led to loose, disaggregated MCs with a smoother outer shell while with lower concentration MCs present a higher degree of aggregation and an irregular outer shell. Figure 3 and 4 show a detailed image of the MCs shell interior. MCs with higher concentration of ibuprofen have a smoother inner shell, where small heterogeneous pores with irregular size can be observed. Lamellar structures with an irregular orientation are detected, more significantly, in the inner and outer shell of IBU_28 MCs which might be attributed to the semicrystalline state of the PCL polymer [36].

Table 2: Microencapsulation yield, Mean diameter and Polydispersity index.

	IBU_16	IBU_28	IBU_34
Encapsulation Yield (%)	58.0	72.1	76.1
Mean Diameter (μm)	69.8 ± 34.2	110 ± 51.1	141.9 ± 60.2
PDI	0.48	0.46	0.42

Figures 5, 6 and 7 display MCs' size distribution which evidence a quite broad size distribution revealing the polydispersity of the MCs. The majority of IBU_16 MCs sizes are comprised between 30 and 110 μm , most of IBU_28 MCs are found between 20-175 μm and IBU_34 MCs between 75 and 200 μm . The higher the concentration of ibuprofen, the larger in size are the MCs, the lower in size polydispersity and higher encapsulation yield. Small MCs are obtained with a low ibuprofen concentration despite the inhomogeneity of the sample in terms of size distribution.

During MCs production, the evaporation of DCM leads to polymer precipitation, enclosing the mate-

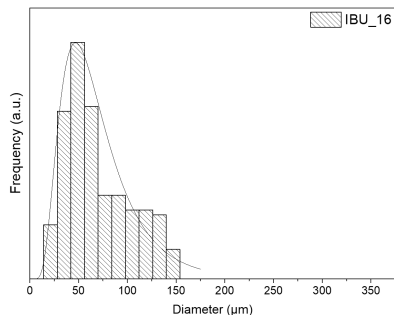


Figure 5: Size distribution of IBU_16 MCs.

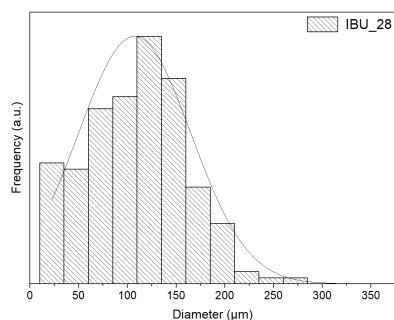


Figure 6: Size distribution of IBU_28 MCs.

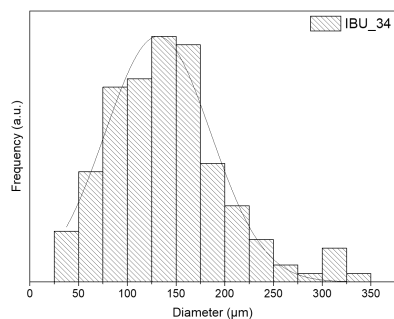


Figure 7: Size distribution of IBU_34 MCs.

rial to be encapsulated in its interior. Therefore, it is assumed that the obtained MCs are only composed by the encapsulated ibuprofen and the precipitated PCL shell, and it is corroborated by FTIR analysis.

Figure 8 shows FTIR spectra of the three MCs produced, of the shell-polymer (PCL) and the encapsulated material (ibuprofen). The FTIR spectrum of ibuprofen contains characteristic bands ca. $1700\text{--}1750\text{ cm}^{-1}$ corresponding to the carbonyl-stretching vibration in hydrogen-bonded dimers [37] while bands between $2950\text{--}2850\text{ cm}^{-1}$ are assigned to C-H vibrations [38]. Other ibuprofen vibrational

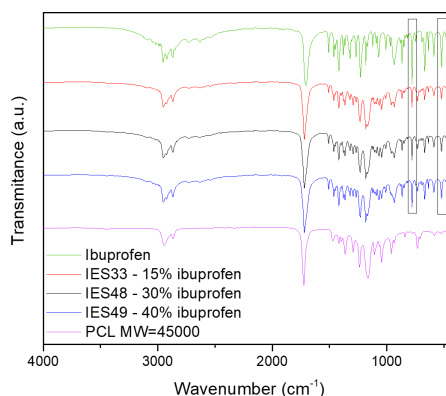


Figure 8: FTIR spectra of the as-prepared MCs (IBU_16, IBU_28 and IBU_34) ibuprofen and the shell-forming polymer (PCL).

stretching bands occur at 1506 cm^{-1} due to C-C vibrational modes in phenyl ring and a band at 780 cm^{-1} attributed to the vibration of C-C groups [38]. Simultaneous detection of these characteristic bands in both ibuprofen and the prepared MCs, proves the presence of ibuprofen in the loaded MCs. The three MCs exhibit an increase of intensity on the previously mentioned peaks, as expected due to the different concentrations of the encapsulated ibuprofen.

TGA analysis were conducted for the two MCs with lower ibuprofen concentration to quantify the encapsulated ibuprofen in the obtained MCs and to corroborate the results obtained from FTIR-ATR.

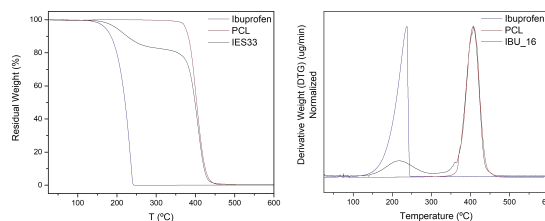


Figure 9: Thermogram of the prepared IBU_16 MCs (left) and respective derivative curves (right).

Figure 9 and 10 show the thermograms and derivative curves of IBU_16 MCs as well as thermograms and DTG of the shell-forming polymer (PCL) and the encapsulated ibuprofen. Ibuprofen and PCL present a well-defined degradation step with a degradation peak of ibuprofen at ca. $75\text{--}250^\circ\text{C}$ and PCL's degradation peak at ca. $350\text{--}450^\circ\text{C}$.

Both samples exhibit an initial degradation step with an onset temperature of ca. 172°C for IBU_16

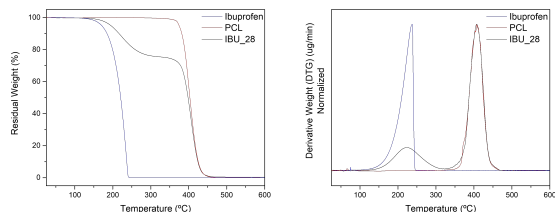


Figure 10: Thermogram of the prepared IBU_28 MCs (left) and respective derivative curves (right).

and ca. 176°C for IBU_28, which correspond to ibuprofen’s degradation. The higher degradation temperature in the MCs’ profile might represent the effect of the MCs’ shell in the degradation of the encapsulated compound. The second degradation step corresponds to the PCL polymeric shell degradation.

Table 3: Encapsulation efficiency of IBU_16 and IBU_28 MCs.

	IBU_16	IBU_28
Mass loss (%) from TGA	15,3	23,6
Theoretical Loading	16	28
Encapsulation Efficiency (%)	95,8	84,4

TGA analysis were conducted to quantitatively determine the encapsulated ibuprofen in the prepared MCs (wt %). The amount of encapsulated ibuprofen, for both MCs, is reported in Table 3. A high degree of encapsulated ibuprofen was obtained, revealing a successful encapsulation by double emulsion system ($W_1/O/W_2$) combined with solvent evaporation method.

Ibuprofen and Calcium Microcapsules

Core-shell microcapsules encapsulating both ibuprofen and calcium were produced by a double emulsion process with solvent evaporation.

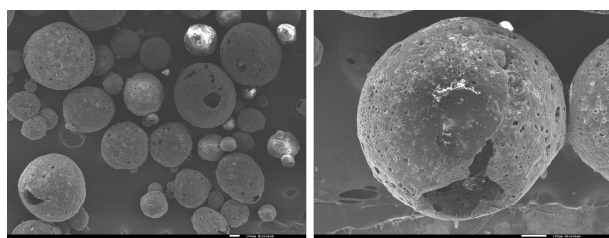


Figure 11: SEM images of IBU_Ca MCs.

Figure 11 shows the SEM photomicrographs of the microcapsules. Spherical and disaggregated microcapsules with core-shell morphology were obtained through this synthesis process. Superficial heterogeneous pores, with irregular size, can be observed in the outer and inner surface.

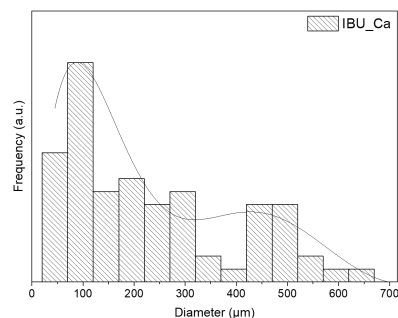


Figure 12: Size distribution of IBU_Ca MCs.

Table 4: Microencapsulation yield, Mean diameter and Polydispersity index.

	IBU_Ca
Encapsulation Yield (%)	55.9
Mean Diameter (µm)	235±169
PDI	0.719

MCs’ size distribution graph shows the polydisperse nature of the microcapsules which is evidenced by the multimodal distribution. The sample presents a very broad size distribution, ranging from 10 to 500 µm, that might be due to the viscosity of the O phase or the less homogeneous oil phase solution which might destabilize the W_1/O emulsion and lead to coalescence during the synthesis process.

Figure 13 shows the FTIR spectra of the prepared MCs as well as the spectra of the shell-forming polymer and the encapsulated ibuprofen and calcium chloride. PLA’s most intense and distinct peak is related to the carbonyl group ($C=O$) stretching vibration at 1746 cm^{-1} . Bands detected at 2995 and 2946 cm^{-1} correspond to $-CH_3$ asymmetric and CH_3 symmetric stretching, respectively. Bands detected in the range of $1500-1350\text{ cm}^{-1}$ are associated with bending vibrations of C-H bonds and the stretching of C-O groups is identified at 1080 cm^{-1} [39].

The analysis of ibuprofen’s FTIR spectrum shows an intense and well defined band at 1720 cm^{-1} attributed to carbonyl-stretching vibrations [37] and at ca. $2950-2850\text{ cm}^{-1}$ to the vibration of C-H groups [38]. Vibrational stretching bands of ibuprofen at 1506 cm^{-1} corresponds to C-C vibrational modes in phenyl rings and the band at 780 cm^{-1} is attributed to the vibration of C-C groups [38]. The simultaneous detection of these characteristic bands in both ibuprofen and the prepared microcapsules, confirms the presence of ibuprofen in the loaded MCs.

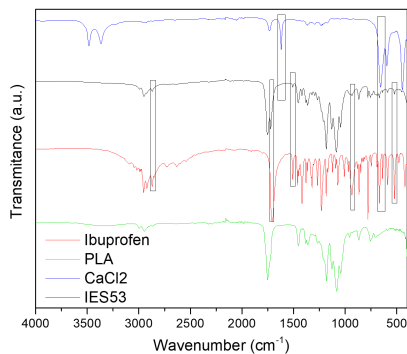


Figure 13: FTIR spectra of IBU_Ca MCs, ibuprofen, calcium chloride and the shell-forming polymer (PLA).

Drug release

The drug release test was performed in order to quantitatively determine the encapsulated material by UV/Vis spectroscopy and Atomic Absorption Spectroscopy. The release profiles depicted in fig-

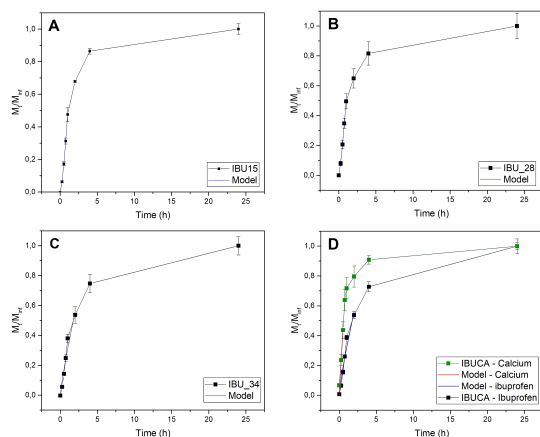


Figure 14: Release profiles of the five prepared microcapsules during a 24h period.

ure 14 show a high burst release of ibuprofen immediately after immersion in the aqueous medium with the release of approximately 80% of the encapsulated content within the initial 5 hours. Plot D in Figure 14 illustrates the release profile of encapsulated ibuprofen and calcium. An initial burst release of both components is observed. After 5 hours, ibuprofen has already released 80% of the total amount of encapsulated material. Calcium has a high release immediately after contact with aqueous medium and the total amount of calcium is released up to 5 hours. The release data points were subjected to Korsmeyer–Peppas model, to evaluate the kinetics and release mechanisms of both com-

pounds (ibuprofen and calcium) from the obtained MCs. Using equation 1, the value of the exponent n was calculated. This exponent is indicative of the mechanism of drug release. All microcapsules follow a similar trend. Exponent values over 0.85 for a spherical geometry show that ibuprofen and calcium follow a non-Fickian diffusion mechanism, known as Super Case-II transport. A non-Fickian transport might be due to different factors, such as swelling, structural changes and relaxation, temperature and sample dimension, etc. [40].

Table 5: Estimated parameters (K) and n values obtained from fitting drug release experimental data to power law.

	IBU_16	IBU_28	IBU_34	IBU_Ca (Ibuprofen)	IBU_Ca (Calcium)
K	0.48	0.5	0.31	0.32	0.81
n	1.46	1.28	0.85	0.81	0.89

Electrochemical Impedance Spectroscopy

Further characterization of the prepared MCs was performed to test their behaviour when in contact with the Mg1Ca alloy. Impedance tests were performed on bare Mg1Ca alloys immersion in three different media: MEM, PBS and NaCl. For the desired application, MEM is the medium that best resembles the conditions inside the human body. The results obtained do not reveal any clear effect or trends associated with the presence of the microcapsules and ibuprofen. The composition of the electrolyte seems to be more relevant for the degradation of Mg1Ca than the presence of the capsules. This is in agreement with the literature [9].

5. Conclusion

This study describes the development of multifunctional, biodegradable MCs, namely ibuprofen-loaded PCL MCs and ibuprofen and calcium-loaded PLA MCs. Microencapsulation, via solvent evaporation using double emulsion ($W_1/O/W_2$) was used. SEM and Optical Microscopy analysis led to the conclusion that lower polymer concentrations (16.7 wt%), higher volume ratio of aqueous phase W_2 and higher concentration of surfactants (4wt% PVA and GA) resulted in less agglomerated and smaller MCs. FTIR results showed the presence of the encapsulated compounds and the correspondent polymer. A high encapsulation efficiency was obtained: 95.8 % and 84.4 % for IBU 16 and IBU 28, respectively. Drug release analysis show a non-Fickian diffusion mechanism of release of both components. EIS results exhibit no negative effect of the presence of MCs on the corrosion behaviour of Mg1Ca alloy in the different media, which reveals that the prepared MCs might be a promising anti-inflammatory strategy, when incorporated within coatings of the metallic biodegradable implants.

Acknowledgements

The author would like to thank her supervisors Dr. Ana Clara Marques and Dr. João Tedim, as well as the colleagues of CERENA and of CICECO groups.

References

- [1] A. K. Nasution and H. Hermawan, *Degradable Biomaterials for Temporary Medical Implants - Biomaterials and Medical Devices, Advanced Structured Materials 58*. Springer International Publishing Switzerland, 2016, doi:10.1007/978-3-319-14845-8.6.
- [2] S. Agarwal, J. Curtin, B. Duffy, and S. Jaiswal, "Biodegradable magnesium alloys for orthopaedic applications: A review on corrosion, biocompatibility and surface modifications," *Materials Science and Engineering C* 68:948–963, 2016.
- [3] M. Salahshoor and Y. Guo, "Biodegradable orthopedic magnesium-calcium (mgca) alloys, processing, and corrosion performance," *Materials (Basel)*; 5(1): 135–155, 2012, doi: 10.3390/ma5010135.
- [4] B.Saad and U.W.Suter, "Encyclopedia of materials: Science and technology (second edition) pages 551-555," 2001, <https://doi.org/10.1016/B0-08-043152-6/00105-4>.
- [5] P. Rocha, "Understanding corrosion mechanisms of novel biodegradable magnesium alloys," Master's thesis, Univ. of Aveiro, 2016.
- [6] Y. Zheng, X. Gu, and F. Witte, "Biodegradable metals," *Materials Science and Engineering: R: Reports* 77:1-34, 2014.
- [7] M. D. Declan Devine Yuanyuan Chen, Marcelo Jorge De Sá and D. M. Devine, *Bioresorbable Polymers - Biodegradable medical implants, pp.17-46*, 2019, <https://doi.org/10.1515/9783110640571-002>.
- [8] M. K. MaHale, N. M. Bergmann, and J. L. West, "Handbook of stem cells (second edition) - chapter 78 - histogenesis in three-dimensional scaffolds, 78(2):951-963," 2013, <https://doi.org/10.1016/B978-0-12-385942-6.00078-0>.
- [9] C.S.Neves, I.Sousa, M.A.Freitas, L.Moreira, C.Costa, J.P.Teixeira, S.Fraga, E.Pinto, A.Almeida, N.Scharnagl, M.L.Zheludkevich, M.G.S.Ferreira, and J.Tedim, "Insights into corrosion behaviour of uncoated mg alloys for biomedical applications in different aqueous media," *J. of Materials Research and Technology* 13:1908-1922, 2021, <https://doi.org/10.1016/j.jmrt.2021.05.090>.
- [10] M. Staigera, A. Pietaka, J. Huadmaia, and G. Diasb, "Magnesium and its alloys as orthopedic biomaterials: A review," *Biomaterials* 27:1728–1734, 2006, doi:10.1016/j.biomaterials.2005.10.003.
- [11] S. Ghosh, Ed., *Functional Coatings and Microencapsulation: A General Perspective*. Wiley-VCH Verlag GmbH, 2006, ch. 1:1-28.
- [12] L. Li, L. Cui, R. Zeng, S. Li, X. Chen, Y. Zheng, and M. Kannan, "Advances in functionalized polymer coatings on biodegradable magnesium alloys – a review," *Acta Biomaterialia* 79:23–36, 2018.
- [13] R. Dubey, T. Shami, and K. B. Rao, "Microencapsulation technology and applications," *Defence Science Journal*, 59(1):82-95, 2009.
- [14] S. Kumari and A. B. and P.K Sharma, "Solvent evaporation as a imposing method for microencapsulation - a review," *Journal of Drug Discovery and Therapeutics* 2(19):13-20, 2014.
- [15] H. Lee, D. Y. Lee, Y.-S. Song, and B.-Y. Kim, "Poly(ϵ -caprolactone) microcapsule with encapsulated nifedipine prepared by magnetic stirrer," *J. Biomedical Engineering Research* 40:7-14, 2019. [Online]. Available: https://www.researchgate.net/publication/331950811_Polye-caprolactone_Microcapsule_wit_h_Encapsulated_Nifedipine_Prepared_by_Magnetic_Stirrer
- [16] M. Lengyel, N. Kállai-Szabó, V. Antal, and A. J. L. I. Antal, "Microparticles, microspheres, and microcapsules for advanced drug delivery," *Sci. Pharm.*, 87, 20, 2019, doi:10.3390/scipharm87030020.
- [17] F. Lim, *Biomedical Applications of Microencapsulation, 1st Edition*. CRC Press, 2021.
- [18] D. Poncelet, "Microencapsulation: Fundamentals, methods and applications," *J.P. Blitz and V.M. Gun'ko (eds.), Surface Chemistry in Biomedical and Environmental Science, 23-34*, 2006, doi: 10.1007/1-4020-4741-X.3.
- [19] W. e. a. Zhang, "Controllable fabrication of inhomogeneous microcapsules for triggered release by osmotic pressure." *Advanced Science News, Small-journal* 1903087, 2019, doi: doi.org/10.1002/sml.201903087.
- [20] Y. Brazier, "What to know about ibuprofen?" Accessed 20/02/2021. [Online]. Available:

- <https://www.medicalnewstoday.com/articles/161071#side-effects>
- [21] B. Tita, A. Fulias, G. Bandur, G. Rusu, and D. Tita, "Thermal stability of ibuprofen. kinetic study under non-isothermal conditions," *Rev. Roum. Chim.*; *55(9)*, 553-558, 2010.
- [22] T. G. and M. Kantor, "Ibuprofen," *Annals of Internal Medicine* *91(6)*, 1979, doi: 10.7326/0003-4819-91-6-877.
- [23] Webmd.com, "Ibuprofen oral: Uses, side effects, interactions, pictures, warnings & dosing - webmd," Accessed 20/02/2021. [Online]. Available: <https://www.webmd.com/drugs/2/drug-5166-9368/ibuprofen-oral/ibuprofen-oral/details>
- [24] "Ibuprofen side effects," Accessed 22/04/2021. [Online]. Available: <https://www.drugs.com/sfx/ibuprofen-side-effects.html>
- [25] N. Carreras, V. Acuña, M. Martí, and M. J. Lis, "Drug release system of ibuprofen in pcl-microspheres," *Colloid Polym Sci*, *291:157-165*, 2013, doi: 10.1007/s00396-012-2768-x.
- [26] K. Durbin, "Ibuprofen," Accessed 22/04/2021. [Online]. Available: <https://www.drugs.com/ibuprofen.html>
- [27] S. S. H. Abadi, A. Moin, and G. H. Veerabhadrapa, "Review article: Fabricated microparticles: An innovative method to minimize the side effects of nsaid in arthritis," *Crit Rev Ther Drug Carrier Syst*: *33(5):433-488*, 2016, doi: 10.1615/CritRevTherDrugCarrierSyst.2016016624.
- [28] Y. Xia, "Uniform biodegradable microparticle systems for protein delivery," 2013, dissertation Univ. of Illinois at Urbana-Champaign. [Online]. Available: core.ac.uk/download/pdf/19529919.pdf
- [29] K. Uhrich, S. Cannizzaro, R. Langer, and K. Shakeshef, "Polymeric systems for controlled drug release," *Chem. Rev.*, *99(11):3181-3198*, 1999.
- [30] E. Mathiowitz, Ed., *Encyclopedia of Controlled Drug Delivery, 1st Edition*. Wiley-Interscience, 1999.
- [31] M. Acharya, S. Mishra, R. N. Sahoo, and S. Mallick, "Infrared spectroscopy for analysis of co-processed ibuprofen and magnesium trisilicate at milling and freeze drying," *Acta Chim. Slov.*, *64:45-54*, 2017, doi: 10.17344/acsi.2016.2772.
- [32] E. Sevostianova, "Atomic absorption spectroscopy," <https://web.nmsu.edu/es-evosti/report.htm>, Accessed 20/05/2021.
- [33] T. Brunetti and C. Seibold, "Calcium (ca2+):perkin elmer analyst 200 atomic absorption spectrometer," Accessed 21/05/2021. [Online]. Available: <http://snobear.colorado.edu/cgi-bin/Kiowa/Kiowa.con.pl?ca2.doc.html>
- [34] R. Revie and H. Uhlig, *Corrosion and Corrosion Control An introduction to Corrosion Science and Engineering, 4th Edition*. Wiley-Interscience, John Wiley & Sons, INC, 2008.
- [35] S. M. Bhagyaraj, O. S. Oluwafemi, N. Kalarikkal, and S. Thomas, *Characterization of Nanomaterials - Advances and key characteristics 1st Edition*, 2018.
- [36] M. V. Loureiro, M. Vale, R. Galhano, S. Matos, J. C. Bordado, I. Pinho, and A. C. Marques, "Microencapsulation of isocyanate in biodegradable poly(ϵ -caprolactone) capsules and application in monocomponent green adhesives," *ACS Applied Polymer Materials*, *2(11):4425-4438*, 2020, DOI: 10.1021/ac-sapm.0c00535.
- [37] T. Azais, C. Tourné-Péteilh, F. Aussenac, N. Baccile, C. Coelho, J.-M. Devoisselle, and F. Babonneau, "Solid-state nmr study of ibuprofen confined in mcm-41 material," *Chem. Mater*, *18:6382-6390*, 2006.
- [38] "Advanced subsidiary gce (h032) advanced gce (h432) - data sheet for chemistry a," Oxford Cambridge and RSA. [Online]. Available: <https://www.ocr.org.uk/images/302739-units-h032-and-h432-data-sheet.pdf>
- [39] B. W. Chieng, N. A. Ibrahim, W. M. Z. W. Yunus, and M. Z. Hussein, "Effects of graphene nanoplatelets on poly(lactic acid)/poly(ethylene glycol) polymer nanocomposites." *Polymers*, *6:93-104*, 2014, doi:10.3390/polym6010093.
- [40] G. Sarti, "Fickian and non fickian and non -fickian diffusion in fickian diffusion in solid polymers solid polymers," *DICMA Alma Mater Studiorum Università di Bologna,Italy*, Accessed 12/09/2021. [Online]. Available: https://diffusion.uni-leipzig.de/presentations_DFII/pdf/DFII_Sarti.pdf